CHARACTERISTICS OF THE THERMAL RADIATION OF NONISOTHERMAL REGIONS

E. V. Lapovok and S. I. Khankov

UDC 536.2.621

Analytical equations are derived which describe a distortion of heat radiation characteristics for gray diffuse and black surfaces, bounded by straight lines or circumferences, with linear and parabolic temperature profiles.

In thermophysical studies based on optical pyrometry with a noncontact determination of characteristic (radiation, color, brightness) temperatures [1], an instability of the radiator temperature [2] can produce appreciable errors. Additional difficulties arise for a nonuniform temperature distribution over the radiating surface area, when a superposition of the radiation characteristics of different-temperature regions brings about uncertainties. It is methodically more complicated to carry out investigations and interpret the measurement results in such cases than in the presence of thermal contrasts between adjacent isothermal regions [3, 4].

The current investigation was aimed at studying the salient features of the radiation characteristics of nonisothermal surfaces, determining the significance criteria of temperature nonuniformities for the simplest configurations of a radiating region with the most typical temperature profiles, correlating the characteristic and surface-average thermodynamic temperatures, and obtaining the effective temperature which defines the radiant energy transfer and characterizes the radiative heat transfer rate.

At the first stage of the investigations, some assumptions and restrictions will be adopted to narrow the range of possible variants of the initial conditions: 1) the radiating surfaces are black or gray diffuse; 2) the regions considered are plane, bounded either by parallel straight lines (a rectangle, an infinite strip) or by a circumference; 3) the observation direction is normal to the plane area and the observation is conducted at a considerable distance, i.e., we assume an almost parallel beam of radiant energy; and 4) temperature distributions of two types are considered, viz., linear and parabolic. Such distributions are typical and can appear in the characteristic heat transfer conditions, i.e., with transverse heat fluxes passing through the section or with a uniform internal heat release. Both processes set up corresponding temperature fields in a stationary thermal mode. Many real situations fall, more or less closely, under the above-stated examples.

1. Let us proceed to considering the heat models of the objects studied (Fig. 1). Spatial orthographic epure projections of linear one-dimensional temperature distributions over a rectangular area (Fig. 1a) and a disk (Fig. 1b) represent the pattern of isotherms depicted by equidistant straight lines.

The temperature distributions in these cases are described by the relations

$$T(\bar{X}) = T_1 + \frac{\Delta T}{2}(1 - \bar{X}),\ \bar{X} = \frac{x}{l}, \tag{1}$$

$$T(\rho,\ \varphi) = T_1 + \frac{\Delta T}{2}(1 + \rho\cos\varphi),\ \rho = \frac{r}{l}, \tag{2}$$

whereas for parabolic temperature distributions (the epures and patterns of isotherms with all necessary designations are given in Fig. 1c, d) we have, correspondingly,

$$T(\bar{X}) = T_1 + \Delta T(1 - \bar{X}^2), \tag{3}$$

All-Union Scientific Center "S. I. Vavilov State Institute for Optics," St. Petersburg. Translated from Inzhenerno-Fizicheskii Zhurnal, Vol. 62, No. 6, pp. 866-872. Original article submitted June 18, 1991.

1062-0125/92/6206-0633$12.50

$$T(\rho) = T_1 + \Delta T(1 - \rho^2). \tag{4}$$

Equations (1)-(4) pertain to the variants of heat models hereinafter numbered in the adopted sequence – accordingly, variants 1-4.

For the convenience of subsequently using Eqs. (1)-(4) in conformity with the physical meaning of the problem, the initial parameters T_1 and ΔT must be substituted by T_s and $\psi = \Delta T/T_s$ (T_s is the surface-average temperature).

The averaging for variants 1 and 3 is executed by one general equation; likewise, a general representation can be assumed for variants 2 and 4:

$$T_s = \frac{1}{2}\int_{-1}^{1} T(\bar{X})\, d\bar{X}, \quad T_s = \frac{1}{\pi}\left(\int_0^1 \rho d\rho\right)^{-1} \int_0^{\pi}\int_0^1 \rho T(\rho, \varphi)\, d\rho d\varphi. \tag{5}$$

Integration yields the expression for T_s that is common for all four variants

$$T_s = T_1 + m\Delta T. \tag{6}$$

The values of m for variants 1-4 are tabulated in Table 1. Having substituted $T_1 = T_s - m\Delta T$ into each of the corresponding Eqs. (1)-(4), we obtain for variants 1-4, accordingly,

$$T(\bar{X}) = T_s\left(1 - \frac{\psi}{2}\bar{X}\right), \quad T(\rho, \varphi) = T_s\left(1 + \frac{\psi}{2}\rho\cos\varphi\right),$$
$$T(\bar{X}) = T_s\left[1 + \frac{\psi}{3}(1 - 3\bar{X}^2)\right], \quad T(\rho) = T_s\left[1 + \frac{\psi}{2}(1 - 2\rho^2)\right]. \tag{7}$$

2. We consider the possible ways to describe the heat radiation of areas, starting from the analysis of the spectral radiation flux density, which for the black surface can be represented as [5]

$$I_\lambda = C_1\lambda^{-5}\left[\exp\left(\frac{C_2}{\lambda T_X}\right) - 1\right]^{-1}, \tag{8}$$

where $C_1 = 0.374\cdot10^{-5}$ W·m^2, $C_2 = 1.4388\cdot10^{-2}$ m·K, and T_X is the temperature which can be specified in two ways: 1) as the surface-average temperature $T_X = T_s$ and then a certain value of $I_{\lambda s}$, corresponding to the radiation of an isothermal black body with a thermodynamic temperature T_s, will be calculated from Eq. (8); 2) as a function of the coordinates, and then I_λ will also be predicted as a function of the appropriate coordinates.

In the latter case, determining the effective value $I_{\lambda e}$, perceived by a detector at a sufficient distance (when the entire radiating region is observed rather than its individual segments), necessitates a numerical integration of function (8) with respect to the appropriate coordinate (or two coordinates for variant 2), which is an argument of this function, whereas T_X becomes an intermediate parameter.

Of particular interest in the problem being solved is investigating the quantity

$$\delta_\lambda = \frac{I_{\lambda e} - I_{\lambda s}}{I_{\lambda s}} \tag{9}$$

as a function of λ, T_s, and ψ.

Having studied the characteristic of the deviation of the radiation spectrum of a nonisothermal area from the radiation spectrum of an isothermal radiator for a black body, it is possible to extend the deductions to the behavior of the same function $\delta_\gamma(\lambda, T_s, \psi)$ for nonblack bodies since the radiation coefficient in the numerator and the denominator of Eq. (9) is cancelled (if insignificant nonlinearities are neglected).

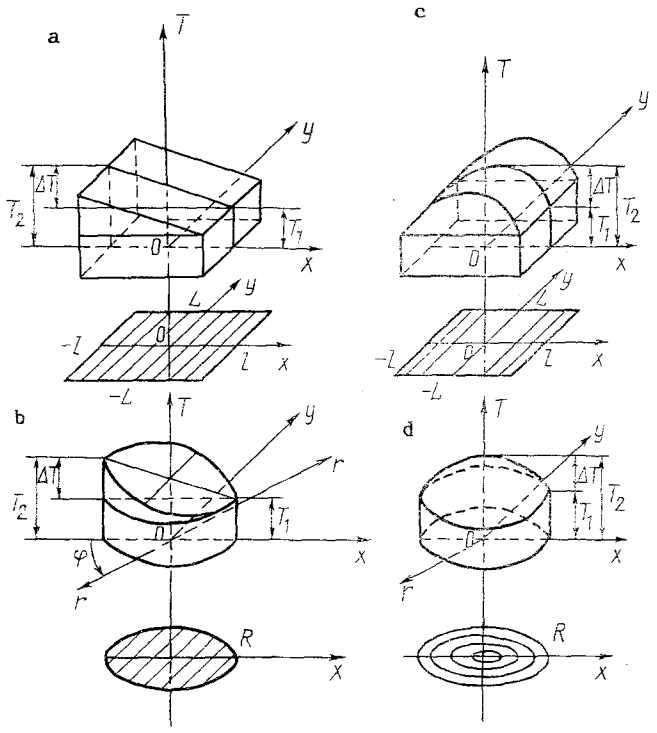

Fig. 1. Heat models of radiating objects: a) linear temperature distribution over a rectangular area, b) linear temperature distribution over a disk; c) parabolic temperature distribution over a rectangular area; d) parabolic temperature distribution in a disk.

For integral radiation, an analogous characteristic δ_Σ is introduced

$$\delta_\Sigma = \frac{E_e - E_s}{E_s}, \tag{10}$$

where, in accordance with the Stefan-Boltzmann law, $E_s = \sigma T_s^4$ [5], and E_e for variants 1 and 3 and separately for variants 2 and 4 can be represented in the corresponding general forms

$$E_e = \frac{\sigma}{2}\int_{-1}^{1} T^4(\bar{X})\,d\bar{X}, \qquad E_e = \frac{\sigma}{\pi}\left(\int_0^1 \rho\,d\rho\right)^{-1}\int_0^{\pi}\int_0^1 \rho T^4(\rho,\ \varphi)\,d\rho d\varphi. \tag{11}$$

3. By the data of numerical studies for all variants 1-4, the quantity δ_λ can be approximated by a unique relation of the form

$$\tilde{\delta}_\lambda = A\zeta^{-2,5}\psi^2, \qquad \zeta = \frac{\lambda T_s}{1000}, \tag{12}$$

where λ is in μm, and $(\lambda T_s)_0 = 1000$ μm·K is taken for convenience. Having assumed here at for each of the variants its own constant value of the proportionality factor A_0 averaged over the range $1 < \zeta < 20$ (such average values are given in Table 1), it is possible to judge the errors of such a simple and convenient approximation from the data of Fig. 2, where $\delta_a = (\delta_\lambda - \tilde{\delta}_\lambda)/\delta_\lambda$ (δ_λ is the relation computed really from Eq. (9) and $\tilde{\delta}_\lambda$ is the approximating function of the form (12)).

As is clear from the figure, the approximation errors for models 1 and 4 are fairly small and do not exceed 10% in the most important range $2 \lesssim \zeta < 10$. For model 2, the errors increase sharply in the same range of ζ but only when $\psi < 0.2$. For variant 3, a peculiarity in the behavior of the approximation errors is observed which is expressed in increased values of δ_a at $\zeta > 5$ and in the curve shapes in the interval $1.5 \lesssim \zeta \leq 4$.

TABLE 1. Parameters of Approximating Equations

Parameter	Variant numbers			
	1	2	3	4
m	1/2	1/2	2/3	1/2
A_0	8,85	6,8	9,5	8,85
ζ_1	1,90	1,85	1,5	1,9
ζ_2	4,75	5,00	4,2	4,75
A_{12}	8,75±0,25	6,6±0,2	$\left(10-\frac{2,6}{\zeta}\right)\pm 0,6$	8,75±0,25
ΔB	620	540	640	620
B_1	2278	2358	2258	2278
b	0,49	0,37	0,54	0,49
D	0,5	0,38	0,5	0,5

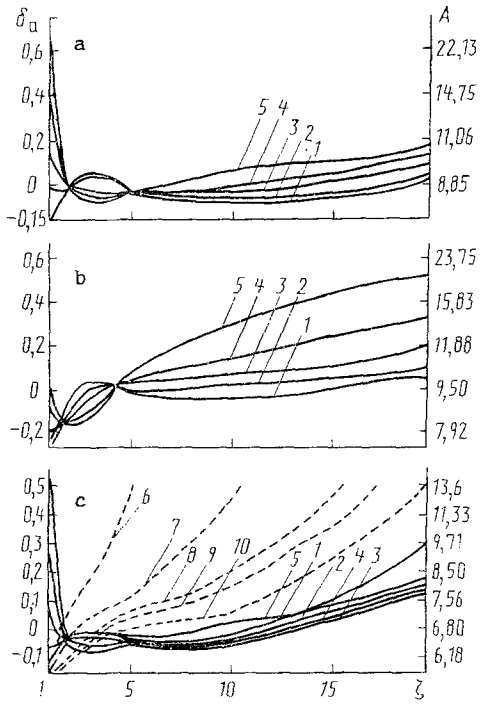

Fig. 2. Relative error of the approximation of δ_a at a constant value of A_0 and values of A as functions of ζ, related to δ_a by $A = A_0/(1 - \delta_a)$: a) models 1 and 4 (Fig. 1a, d); b) model 3 (Fig. 1 c); c) model 2 (Fig. 1 b); 1, ψ = 0.2; 2, 0.4; 3, 0.6; 4, 0.8; 5, 1.0; 6, 0.01; 7, 0.03; 8, 0.05; 9, 0.07; 10, 0.1.

It should be noted that marked errors are characteristic of the sections of little practical importance – in the range $\zeta < 1$ the radiant flux contains a small fraction of the total energy (< 0.1%), whereas for $\zeta > 10$, $\delta_\lambda < 0.1\%$, which is beyond the scope of the metrological capabilities of the measuring equipment. At the same time, for a practically complete elimination of the approximation error, the curves in Fig. 2 can be considered as the relation $A(\zeta)$ (the corresponding values of A on the ordinate axis are given on the right), whereas for a partial but substantial elimination of the error, it is sufficient to narrow the range of ζ studied. Thus, it is evident from Fig. 2 that the curves $\delta_a(\zeta)$ as well as $A(\zeta)$ have intersection points for various ψ. The coordinates of points ζ_1 and ζ_2 are given in the table, which also presents the average values of A_{12} for this range with the indicated maximum deviations from the average value in the chosen range. As can be seen from the data of the table, the approximation error in the most important range $2 < \zeta < 4$-5, containing 50% of the total energy, is, on the average, not larger than about 3%.

In studying the quantity δ_λ, analytical relations for the values that of λ_m as functions of ψ were obtained at which λ reaches an extremal value. With an error less than 1% it can be written that

$$\lambda_m = \frac{B(\psi)}{T_s}, \quad B(\psi) = B_0 - \Delta B\psi^n, \quad \Delta B = B_0 - B_1,$$
$$B_0 = B(\psi = 0), \quad B_1 = B(\psi = 1), \quad n = 2(1 - b\psi). \tag{13}$$

where $B_0 = 2898$ μm·K [3-5] and the values of ΔB, B_1, and b are given in the table. With $\psi = 0$, Eq. (13) goes over into the equation describing the Wien displacement law.

The quantity δ_Σ can be defined using the analytical solution of integrals (5) and (11). In all the four variants we can confine ourselves to the equation

$$\tilde{\delta}_\Sigma = D\psi^2. \tag{14}$$

The values of the proportionality factors D with an error less than 1% for the variants of heat models considered are tabulated.

It is noteworthy that similar results can also be obtained for the characteristics of directed radiation of three-dimensional nonisothermal bodies, i.e., for nonplanar surfaces. As an example, a cylinder with a linear transverse temperature field can be examined. At large distances from the cylinder in the directions normal to the generatrix in the coordinates $\varphi = 0$ and π, $T(\varphi = 0) = T_2$, $T(\varphi = \pi) = T_1$ (see Fig. 1b), the relative deviations of δ_λ and δ_Σ, when approximated by Eqs. (12) and (14), have the following coefficients: A = 1.8 and D = 0.105. At the same time, when the observation is executed from the intermediate position $\varphi = \pi/2$, the values of δ_λ and δ_Σ prove to be identical to those for a plane projection of the same cylinder. In determining the radiation characteristics of such a cylinder in various directions it is possible, in principle, to find in it the characteristic features of the indicated temperature distribution.

4. Let us consider the analogs of the characteristic (radiation, color, and brightness) temperatures used in pyrometry for nonisothermal radiating areas.

Taking into account that the radiation temperature T_r for the black body coincides with its thermodynamic temperature T_T, whereas $E_e = \sigma T_r^4 = \sigma T_T^4$ and $E_s = \sigma T_s^4$, Eqs. (10) and (14) yield

$$T_p = T_r = \sqrt[4]{1 + \delta_\Sigma}\, T_s = \sqrt[4]{1 + D\psi^2}\, T_s \tag{15}$$

and it turns out that the effective thermodynamic (or radiation) temperature governing the specific power of the radiant flux and characterizing the rate of the radiative heat transfer exceeds the surface-average temperature of the radiating area since D > 0. In the limiting hypothetic case $\psi \simeq 1$ for models 1, 3, and 4 we obtain $T_r = 1.105T_s$.

The color temperature can be defined with the aid of Eq. (13):

$$T_c = \left(1 - \frac{\Delta B}{B_0}\psi^n\right)^{-1} T_s \tag{16}$$

and at $\psi \to 1$ for variants 1 and 4 $T_c \simeq 1.272$ T_s.

The expression for the brightness temperature can be derived with consideration of Eqs. (8) and (9); for the range $1 < \zeta < 5$ it is convenient to utilize the relation

$$T_b = \left[1 - \lambda T_s \frac{1}{b}\ln(1 + \delta_\lambda)\right]^{-1} T_s, \tag{17}$$

where $b_0 = (hc)/k = 14 \cdot 10^3$ μm·K.

For $\delta_\lambda < 0.1$, with an error less than 4%,

$$T_b \cong \left(1 - \frac{\zeta}{14}\delta_\lambda\right)^{-1} T_s = \left(1 - \frac{A}{14}\zeta^{-1,5}\psi^2\right)^{-1} T_s. \tag{18}$$

As seen from Eqs. (15)-(18), the characteristic (radiation, color and brightness) temperatures for a nonisothermal region with any of the considered configurations and temperature profiles are higher than the surface-average temperature, which is noticeable, however, for significant temperature nonuniformities at values of ψ close to unity.

5. It is appropriate here to tackle the question as to the criterion of a sufficient isothermality. In case we proceed from the spectral-energy characteristics of radiation and assume the permissible value $\delta_\lambda \simeq 1\%$, then, according to Eq. (12) and the tabulated data, the permissible nonuniformity for variants 1, 3, and 4 constitutes, on the average, $\psi_p \lesssim 0.03\ \zeta^{1.25}$, i.e., at $\zeta \simeq 1$ we have $\psi_p \lesssim 0.03$, whereas at $\zeta = 4$ we obtain already $\psi_p \lesssim 0.15$. For the integral radiation characteristic, taking $\delta_\Sigma \simeq 1\%$, we get for the same variants $\psi_p \lesssim 0.15$. Interestingly, with the allowance for δ_Σ expanded to 10%, the requirements for isothermality reduce appreciably. At the same time, when the range of the permissible distortion of the spectral radiation composition is extended to $\delta_\lambda \simeq 10\%$, the requirements for isothermality remain the more stringent the smaller the value of ζ.

It must be pointed out that, for practical measurements, the energy characteristic in a definite interval of the values of $\Delta\zeta$ can prove to be more interesting. In this case, the deviation of the energy characteristic of radiation from that typical of the black body can be found through integrating Eq. (12):

$$\delta_{\Delta\zeta} = \frac{1}{\zeta_2 - \zeta_1} \int_{\zeta_1}^{\zeta_2} \delta_\zeta d\zeta = \frac{2}{3} \frac{A\psi^2}{\zeta_2 - \zeta_1} \left(\frac{1}{\sqrt{\zeta_1^3}} - \frac{1}{\sqrt{\zeta_2^3}} \right). \tag{19}$$

As an example, consideration will be given to three characteristic ranges of ζ: 1-4, 4-8, and 4-16 (the first and third ranges contain up to half the total radiation power). With $\psi = 0.2$, the values of $\delta_{\Delta\zeta}$ in these ranges are equal, accordingly, to 7, 0.5, and 0.25% (in calculations, the average value of A for variants 1, 3, and 4 is taken). While the deviation in the first range can be observed, the nonisothermality signs in the second and third ranges of ζ will not be noticeable actually with any measurement method used.

6. To the most interesting conclusions ensuing from the results of the investigations conducted, it is possible to refer the possibility of discriminating, under definite conditions, the characteristic configuration of the radiating area and the typical temperature profile on its surface. In this regard, variants 1 and 4 turn out to be identical, which is determined from the similarity of the results of averaging the parameters governing the values of δ_λ and δ_Σ. Variant 3 is characterized by an elevated, as compared with others, value of T_s relative to T_1 and ΔT (see Eq. (6) and the table), which leads to an increase in the values of δ_λ and to a displacement of the interval ζ_2-ζ_1 towards smaller values with increasing coefficient A over the interval (ζ_1, ζ_2) (see the table). Variant 2 differs strongly from the remaining ones by the minimum deviation of the radiation characteristics from the case with an isothermal surface (by the minimum values of A and D, see the table). This becomes physically understandable provided an account is taken of the fact that, as compared with variant 1, in the variant 2 model the regions with the temperature other than the surface-average temperature have a smaller weight (take up smaller areas). Here, the coefficients A and D for variants 1 and 2 relate in approximately the same way as the area of a square to the area of a circle inscribed in it.

The derived analytical equations provide, regardless of their simplicity, effective estimates of the distortion of the radiation characteristics resulting from the surface nonisothermality. The considered approach can be extended to more complex variants of the heat models of objects.

NOTATION

T, temperature of radiating surface, K; T_1, minimum temperature of radiating surface, K; ΔT, temperature drop on radiating surface, K; T_s, surface-average temperature, K; T_T, T_c, and T_b, thermodynamic, color, and brightness temperatures; X, r, and φ, running coordinates; l, characteristic dimension, m; I_λ, surface-average radiation flux density, $W/(m^2 \cdot \mu m)$; λ, wavelength, μm; λ_m, the value of λ at which surface-average radiation flux density takes the extreme value, μm.

LITERATURE CITED

1. G. S. Landsberg. Optics [in Russian], Moscow (1976).
2. A. G. Maki and E. K. Plyler, J. Res. Nat. Bur. Standards, **66**, No. 3, 283-287 (1962).
3. M. M. Miroshnikov, Theoretical Principles of Optical-Electronic Instruments [in Russian], Leningrad (1983).

4. Zh. Gossorg, Infrared Thermography. Principles, Techniques, Application [in Russian], Moscow (1988).
5. G. N. Dul'nev and E. M. Semyashkin, Heat Transfer in Radioelectronic Apparatus [in Russian], Leningrad (1968).

LOCAL CHARACTERISTICS OF HEAT-RADIATION SUPERCONDUCTOR DETECTORS BASED ON HIGH-TEMPERATURE SUPERCONDUCTOR FILMS

O. S. Esikov, A. I. Krot, I. G. Merinov, E. A. Protasov, V. P. Sobolev, and V. S. Kharitonov

UDC 536.3: 621.317.794

Relations are proposed for evaluating the local values of the thermal sensitivity, speed of response, and resolution of a heat radiation detector based on high-temperature superconductor films.

Superconductor sensitive elements (SE) find an ever wider application in creating heat radiation detectors [1]. Until recently, however, their application has been limited by the necessity of using liquid helium as a thermostabilizing coolant. The appearance of high-temperature superconductors (HTSC), whose superconducting transition temperature exceeds the boiling temperature of liquid nitrogen at normal pressure, has greatly extended the range of application of superconductive heat radiation detectors (SHRD). Study [2] analyzed the integral inertial-sensitive characteristics of SHRD manufactured based on HTSC films by various methods of their thermostabilization. It is shown that they are determined chiefly by the thermophysical properties of the substrate and by the value of the thermal coupling of the SE with the thermostat. The estimates obtained therein made it possible to draw a conclusion that the existing technologies permit the creation, based on HTSC films, of SEs operating at nitrogen temperatures, which could provide, with response times of about 1 sec, integral thermal response not worse that 10^3 K/W.

The detection of several heat radiation sources or the image reconstruction of an extended heat source raises the problems of the spatial and temporal resolution of heat fluxes incident on SE. The local thermal characteristics of the SEs of SHRDs also begin to play an important role. The aim of the present study is to analyze the basic local thermal characteristics (sensitivity, speed of response, and resolution) of the SEs of SHRDs based on HTSC films.

In the simplest of cases an SE is a flat multilayer structure whose main elements are an HTSC film, a substrate, a thermally-controlled coolant duct, and a thermal resistance providing for the thermal coupling of the substrate with the coolant duct (Fig. 1). The thickness of the HTSC film is usually two orders of magnitude smaller than the substrate thickness and is about 1 μm. Therefore, already 1 μsec after heat radiation starts affecting the SE, the substrate influence on a temperature mode of the HTSC film becomes dominant. To estimate local thermal characteristics of the SE, let us substitute for it a model of a semi-infinite medium with the same thermophysical parameters as the substrate and analyze its temperature field due to a narrowly-directed heat radiation flux incident on the surface (Fig. 2).

To describe the substrate temperature in the approximation adopted, we can use the known solution to a problem on the propagation of thermal energy into the half-space from the local heat source of power Q located on its surface in a circle of radius r_0 [3]:

$$\Delta T(r,\ z,\ t) = T(r,\ z,\ t) - T_0 = \frac{Q}{2\pi r_0 \lambda} \int_0^\infty J_0(\xi r)\, J_1(\xi r_0) \times \left(\exp(\xi z)\, \Phi\left(\frac{z}{2(at)^{0,5}} + \xi (at)^{0,5} \right) - \right.$$
$$\left. - \exp(-\xi z)\, \Phi\left(\frac{z}{2(at)^{0,5}} - \xi (at)^{0,5} \right) - 2\,\mathrm{sh}(\xi z) \right) \frac{d\xi}{\xi}. \qquad (1)$$

Moscow Institute of Engineering Physics. Translated from Inzhenerno-Fizicheskii Zhurnal, Vol. 62, No. 6, pp. 873-877. Original article submitted July 30, 1991.